Microwave transitions in “geonium”

ν_c~150 GHz

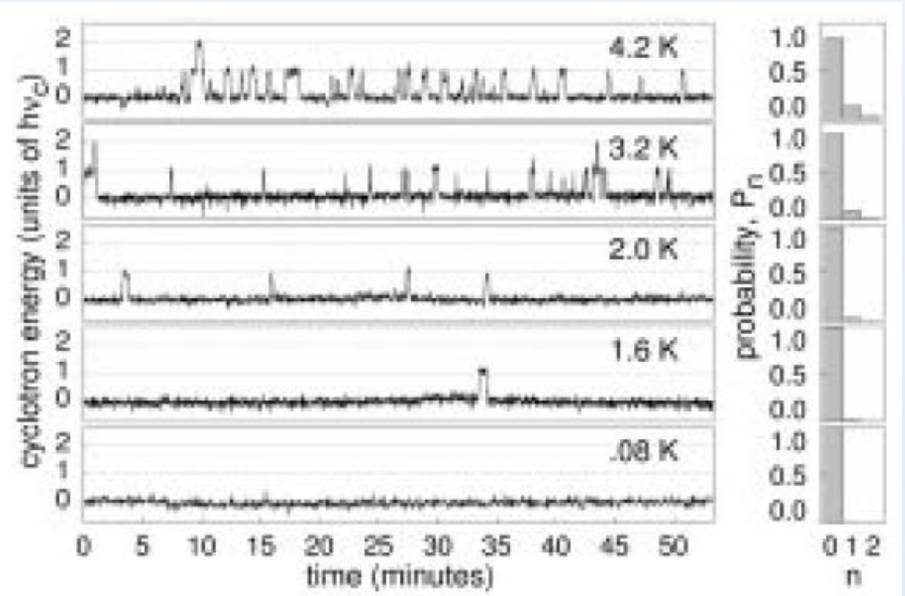

FIG. 2. Quantum jumps between the lowest states of the one-electron cyclotron oscillator decrease in frequency as the cavity temperature is lowered.

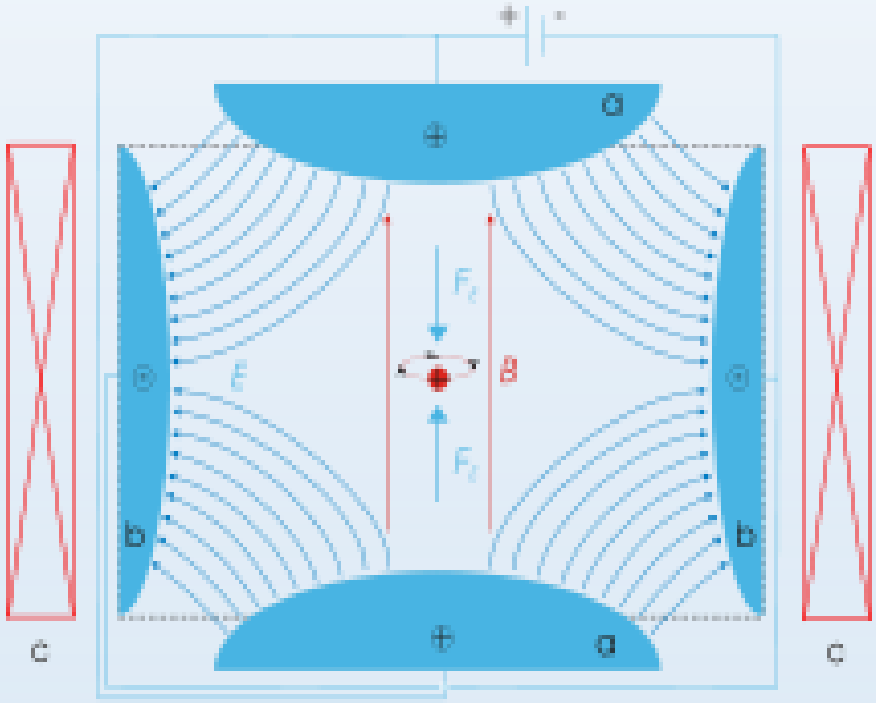

proton trapped in Penning trap
(B-field + repulsive endplates)

Observing the Quantum Limit of an Electron Cyclotron: QND Measurements of Quantum Jumps between Fock States

S. Peil and G. Gabrielse

Department of Physics, Harvard University, Cambridge, Massachusetts 02138

(Received 18 March 1999)

Microwave transitions in “geonium”

ν_c~150 GHz

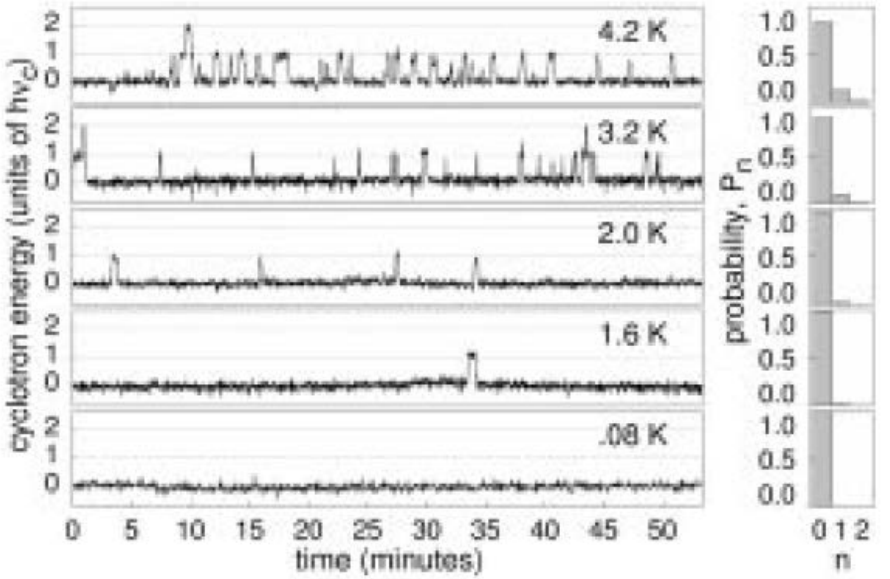

FIG. 2. Quantum jumps between the lowest states of the one-electron cyclotron oscillator decrease in frequency as the cavity temperature is lowered.

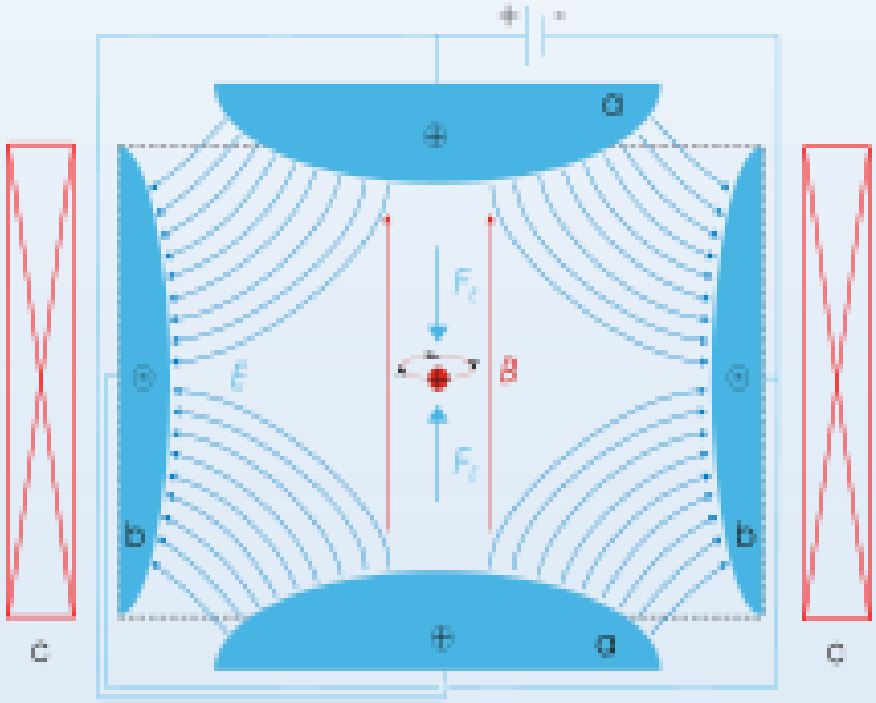

proton trapped in Penning trap
(B-field + repulsive endplates)

How can we operate most AMO experiments at room temperature, without blackbody radiation mucking things up?
(typical ground-state hyperfine level splittings ~ GHz)

Microwave transitions in “geonium”

ν_c~150 GHz

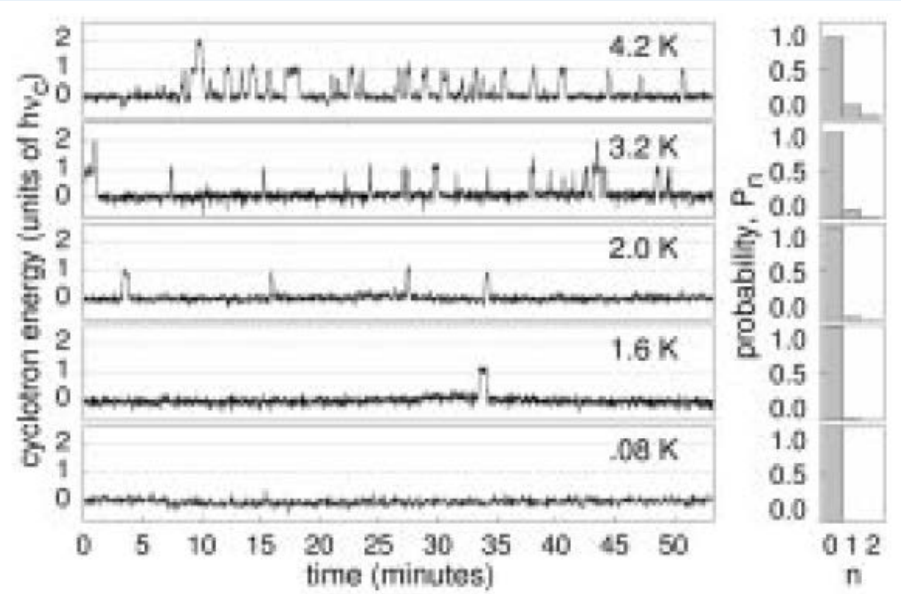

FIG. 2. Quantum jumps between the lowest states of the one-electron cyclotron oscillator decrease in frequency as the cavity temperature is lowered.

Main reason – selection rules!

The electron is changing parity when it gets excited between geonium levels, hence dipole-allowed.

The transitions at these frequencies in atoms are typically $\Delta l = 0$, and thus electric-dipole forbidden

One factor: less blackbody radiation at MHz to few GHz range

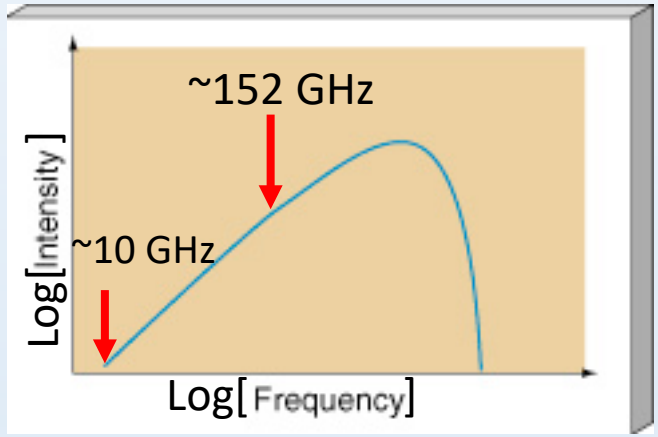

$$B_\nu(\nu,T) = \frac{2h\nu^3}{c^2}\frac{1}{e^{\frac{h\nu}{k_B T}} - 1}$$

Second factor: transition rate of scales like ν^3

→ much smaller for few GHz vs. 150 GHz

Finishing up from last time…

the cesium fountain clock > maser

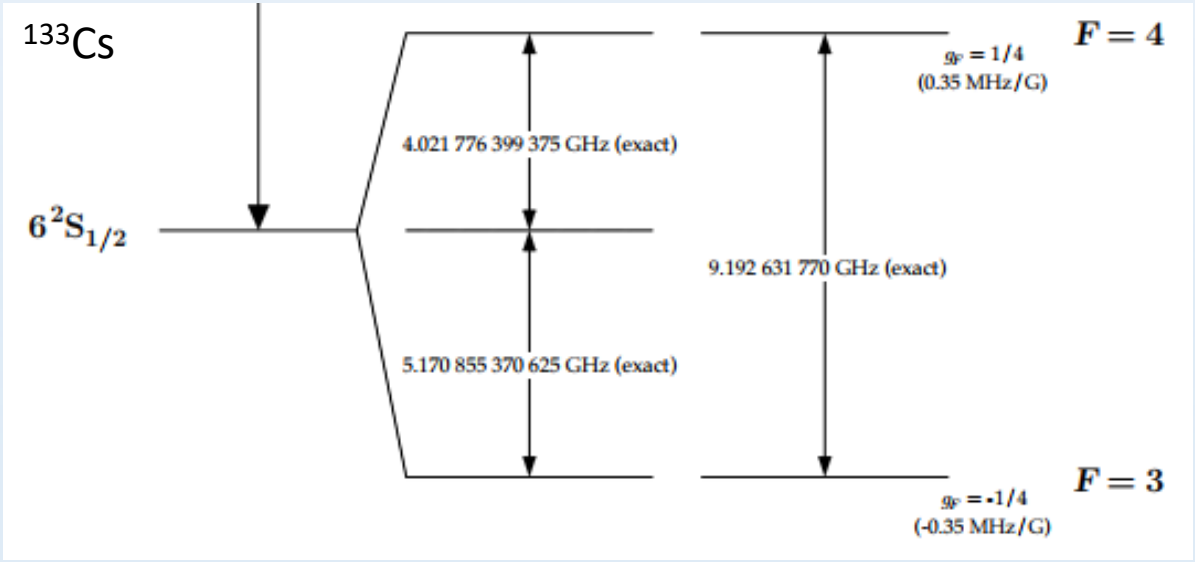

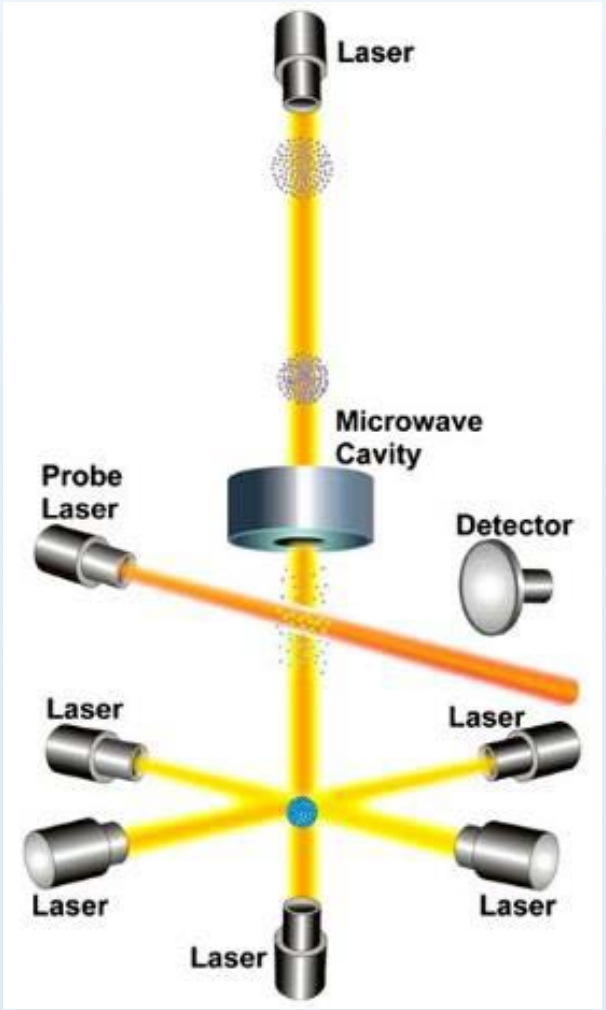

ΔE determines the SI second (and meter)

Finishing up from last time…

the cesium fountain clock > maser

NIST F1

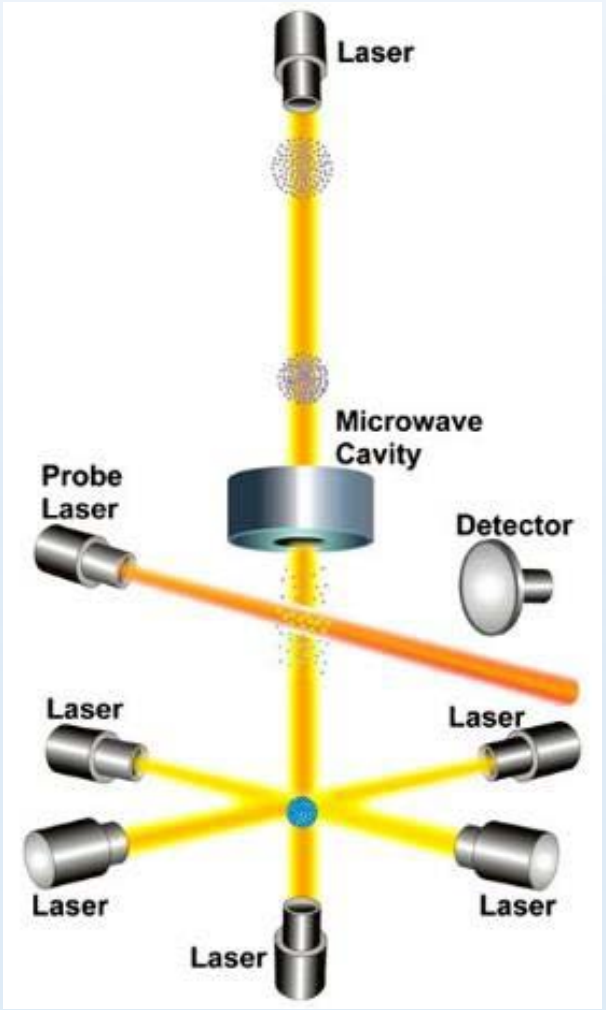

ΔE determines the SI second (and meter)

Finishing up from last time…

Hyperfine level splitting ≠ A_{hfs} (unless it does)

9.192 631 770 GHz (exact)

$$H_{hfs} = hA_{hfs}\frac{\vec{I}\cdot\vec{J}}{\hbar^2}$$

Interval rule: $E_{F+1} - E_F = (F+1)hA_{hfs}$

Element	Abundance	I	F_g (J_g=1/2)	A (MHz)	ΔE_{fs} (GHz)	F_e (J_e=1/2)	A (MHz)	F_e (J_e=3/2)	A (MHz)	B (MHz)
^{1}H	99.985	1/2	0,1	1420.405	10.968	0,1	59.18	1,2	23.67	–
^{6}Li	7.5	1	1/2,3/2	152.137		1/2,3/2	17.375	1/2,3/2,5/2	−1.155	−0.10
^{7}Li	92.5	3/2	1,2	401.752	10.091	1,2	45.914	0,1,2,3	−3.055	−0.221
^{23}Na	100	3/2	1,2	885.813	515.53	1,2	94.3	0,1,2,3	18.69	2.90
^{39}K	93.26	3/2	1,2	230.859	1730.4	1,2	28.85	0,1,2,3	6.06	2.83
^{40}K	0.0117	4	7/2,9/2	−285.731		7/2,9/2	–	5/2,7/2,9/2,11/2	−7.59	−3.5
^{41}K	6.73	3/2	1,2	127.007		1,2	–	0,1,2,3	3.40	3.34
^{85}Rb	72.17	5/2	2,3	1011.910	7123.0	2,3	120.72	1,2,3,4	25.009	25.88
^{87}Rb	27.83	3/2	1,2	3417.341		1,2	406.2	0,1,2,3	84.845	12.52
^{133}Cs	100	7/2	3,4	2298.157	16611.8	3,4	291.90	2,3,4,5	50.34	−0.38

TABLE C.4. Fine- and hyperfine structure constants for the various alkali-metal atoms. The parameters A and B can be used in Eqs. 4.2 and 4.3 to calculate the shift and the splitting from the hyperfine interaction. The values for A and B are from Ref. 28.

Metcalf & van der Straten, Laser Cooling and Trapping

Finishing up from last time…

Hyperfine level splitting ≠ A_{hfs} (unless it does)

9.192 631 770 GHz (exact)

$$H_{hfs} = hA_{hfs}\frac{\vec{I}\cdot\vec{J}}{\hbar^2}$$

Interval rule: $E_{F+1} - E_F = (F+1)hA_{hfs}$

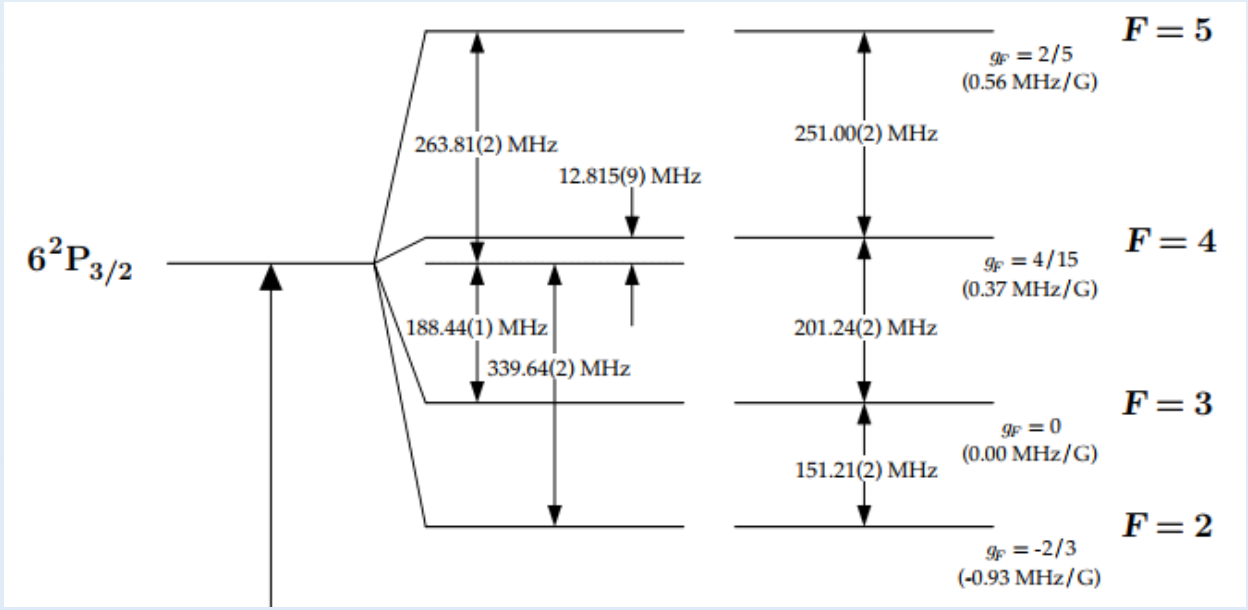

A (MHz)	B (MHz)
23.67	–
−1.155	−0.10
−3.055	−0.221
18.69	2.90
6.06	2.83
−7.59	−3.5
3.40	3.34
25.009	25.88
[illegible]	12.52
50.34	−0.38

sed in Eqs. 4.2 and 4.3 to

Metcalf & van der Straten, Laser Cooling and Trapping

Lecture 6: Atoms in static (B) fields

Readings: Foot Chapter 6.3-6.4

So far: structure native to the atom

- electrostatic interactions
- interactions of electron and nuclear spins with
  (a) other spins and
  (b) effective fields due to motion of charged particles

The terms $H_{S-O} \propto \vec{S} \cdot \vec{L}$ and $H_{hfs} \propto \vec{I} \cdot \vec{J}$ reduce symmetry, break degeneracies

- For the simple hydrogen model, ignoring shielding and these terms, all m_L, m_S, and m_I combos are degenerate
- Today we'll talk about the limit of a **strong** B-field applied along a particular direction (quantization axis, $\hat{z}$), breaking the symmetry of the problem and choosing these quantum numbers (relating to states with pure, quantized angular momentum w.r.t. $\hat{z}$)

The Zeeman effect

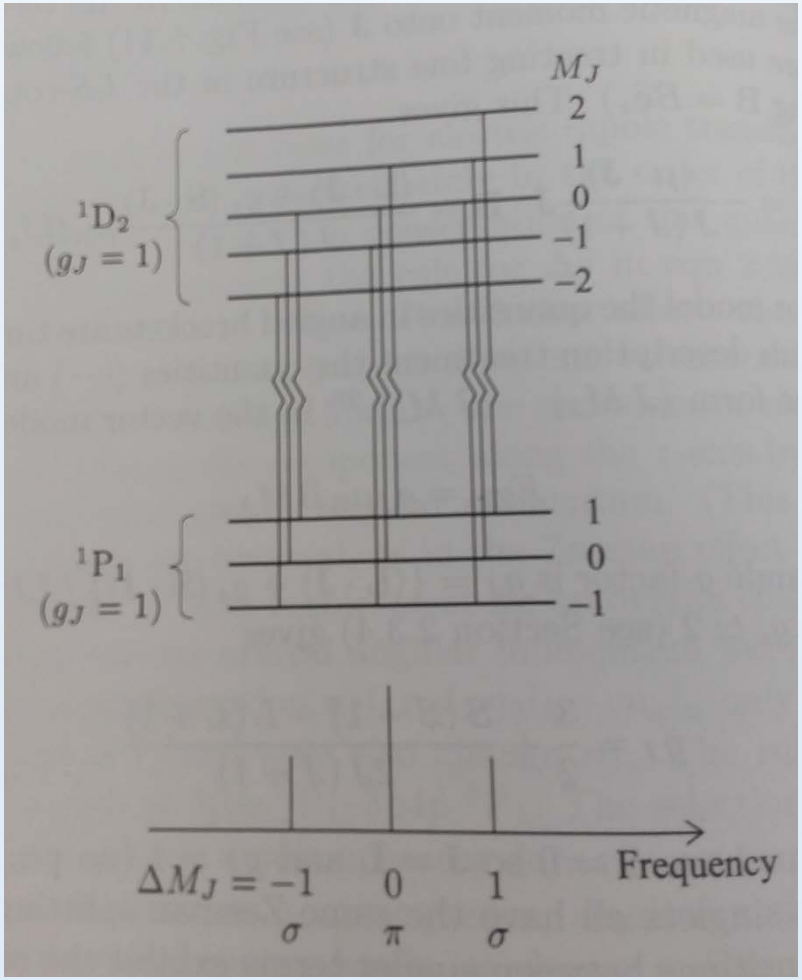

Normal Zeeman effect

Sodium D1 in weak fields
(anomalous Zeeman effect)

Foot

$L \cdot S$ coupling – how high is high?

Element	Abundance	I	F_g ($J_g = 1/2$)	A (MHz)	ΔE_{fs} (GHz)	F_e ($J_e = 1/2$)	A (MHz)	F_e ($J_e = 3/2$)	A (MHz)	B (MHz)
^{1}H	99.985	1/2	0,1	1420.405	10.968	0,1	59.18	1,2	23.67	–
^{6}Li	7.5	1	1/2, 3/2	152.137		1/2, 3/2	17.375	1/2, 3/2, 5/2	−1.155	−0.10
^{7}Li	92.5	3/2	1,2	401.752	10.091	1,2	45.914	0,1,2,3	−3.055	−0.221
^{23}Na	100	3/2	1,2	885.813	515.53	1,2	94.3	0,1,2,3	18.69	2.90
^{39}K	93.26	3/2	1,2	230.859	1730.4	1,2	28.85	0,1,2,3	6.06	2.83
^{40}K	0.0117	4	7/2, 9/2	−285.731		7/2, 9/2	–	5/2, 7/2, 9/2, 11/2	−7.59	−3.5
^{41}K	6.73	3/2	1,2	127.007		1,2	–	0,1,2,3	3.40	3.34
^{85}Rb	72.17	5/2	2,3	1011.910	7123.0	2,3	120.72	1,2,3,4	25.009	25.88
^{87}Rb	27.83	3/2	1,2	3417.341		1,2	406.2	0,1,2,3	84.845	12.52
^{133}Cs	100	7/2	3,4	2298.157	16611.8	3,4	291.90	2,3,4,5	50.34	−0.38

TABLE C.4. Fine- and hyperfine structure constants for the various alkali-metal atoms. The parameters A and B can be used in Eqs. 4.2 and 4.3 to calculate the shift and the splitting from the hyperfine interaction. The values for A and B are from Ref. 28.

Metcalf & van der Straten, Laser Cooling and Trapping

Low-field splitting
Lamb shift measurement – $2S_{1/2} \rightarrow 2P_{3/2}$

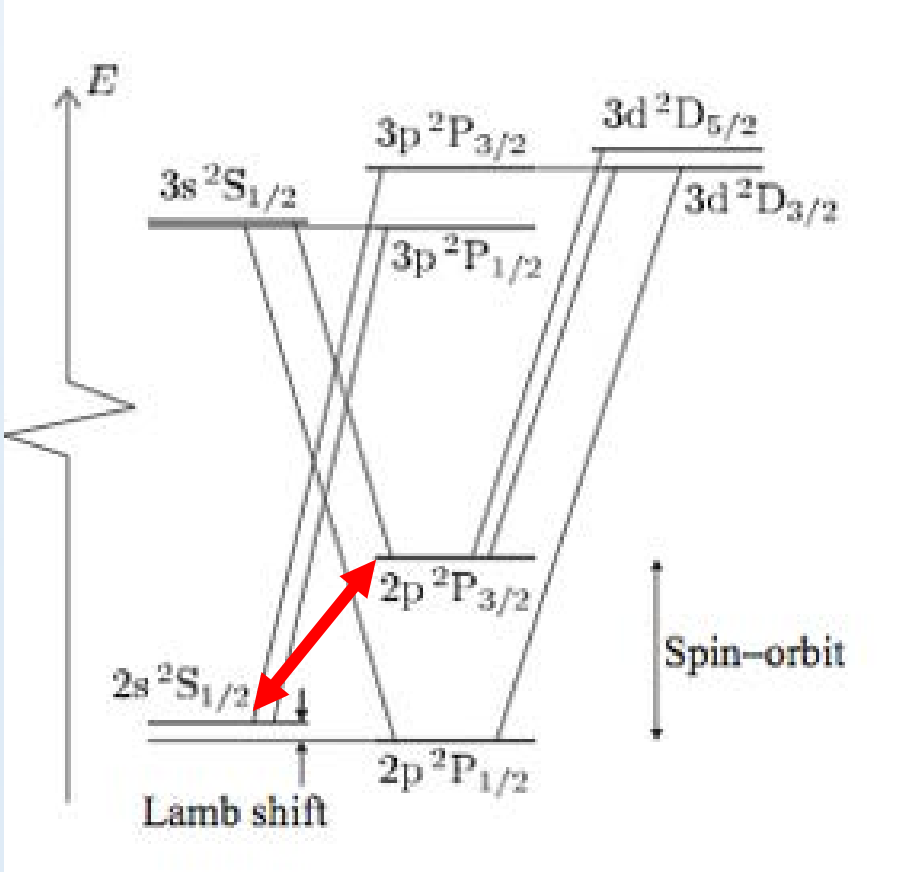

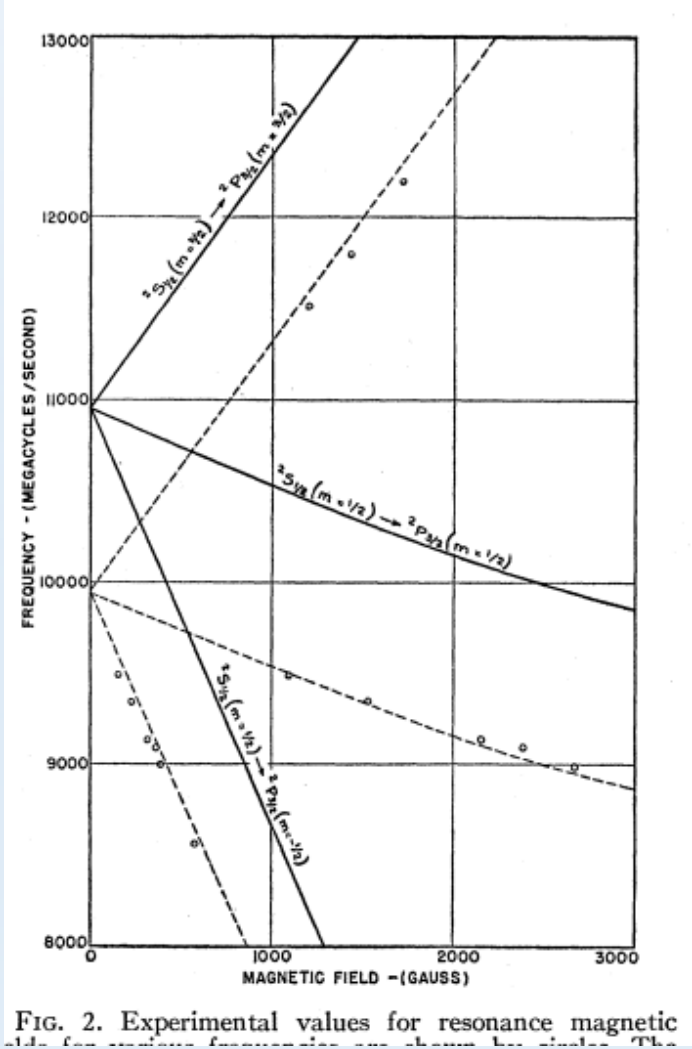

FIG. 2. Experimental values for resonance magnetic

$I \cdot J$ coupling – how high is high?

Element	Abundance	I	F_g ($J_g = 1/2$)	A (MHz)	ΔE_{fs} (GHz)	F_e ($J_e = 1/2$)	A (MHz)	F_e ($J_e = 3/2$)	A (MHz)	B (MHz)
^{1}H	99.985	1/2	0,1	1420.405	10.968	0,1	59.18	1,2	23.67	–
^{6}Li	7.5	1	1/2, 3/2	152.137		1/2, 3/2	17.375	1/2, 3/2, 5/2	−1.155	−0.10
^{7}Li	92.5	3/2	1,2	401.752	10.091	1,2	45.914	0,1,2,3	−3.055	−0.221
^{23}Na	100	3/2	1,2	885.813	515.53	1,2	94.3	0,1,2,3	18.69	2.90
^{39}K	93.26	3/2	1,2	230.859	1730.4	1,2	28.85	0,1,2,3	6.06	2.83
^{40}K	0.0117	4	7/2, 9/2	−285.731		7/2, 9/2	–	5/2, 7/2, 9/2, 11/2	−7.59	−3.5
^{41}K	6.73	3/2	1,2	127.007		1,2	–	0,1,2,3	3.40	3.34
^{85}Rb	72.17	5/2	2,3	1011.910	7123.0	2,3	120.72	1,2,3,4	25.009	25.88
^{87}Rb	27.83	3/2	1,2	3417.341		1,2	406.2	0,1,2,3	84.845	12.52
^{133}Cs	100	7/2	3,4	2298.157	16611.8	3,4	291.90	2,3,4,5	50.34	−0.38

TABLE C.4. Fine- and hyperfine structure constants for the various alkali-metal atoms. The parameters A and B can be used in Eqs. 4.2 and 4.3 to calculate the shift and the splitting from the hyperfine interaction. The values for A and B are from Ref. 28.

Metcalf & van der Straten, Laser Cooling and Trapping

$I \cdot J$ coupling – how high is high?

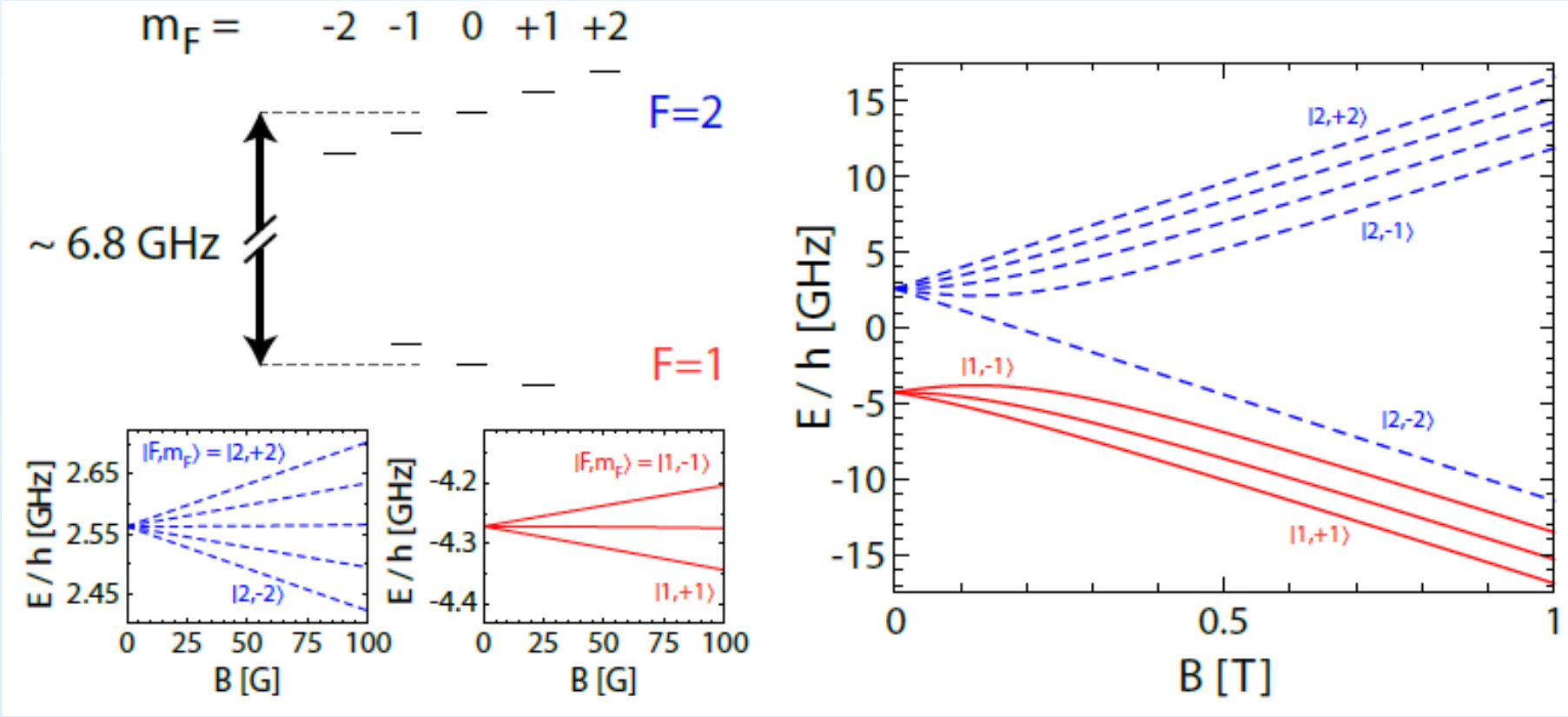

rubidium-87, 6.8 GHz splitting

Note that that the magnetic moment actually depends on the field:

- it can become zero, change signs, etc. as low-field states become mixed

$$\mu = \frac{\partial E}{\partial B}$$

$I \cdot J$ coupling – how high is high?

high field happens at much lower fields, ~ tens of G

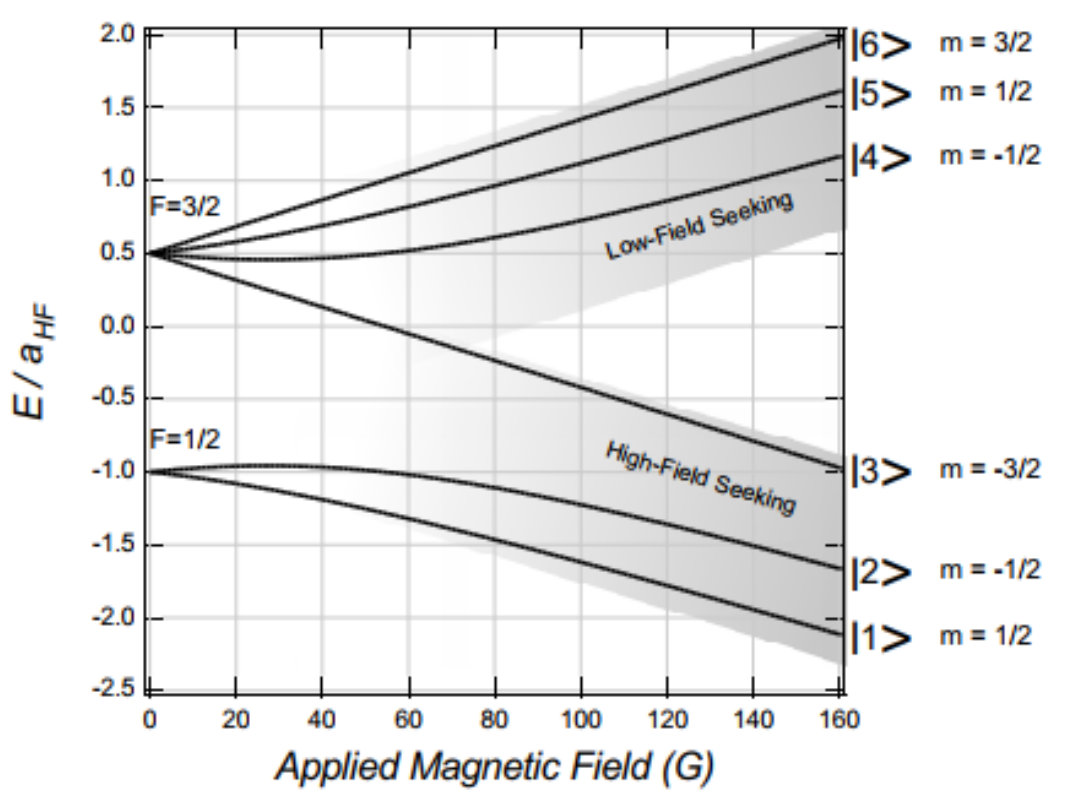

lithium-6, 150 MHz splitting

Michael Gehm

$I \cdot J$ coupling – how high is high?

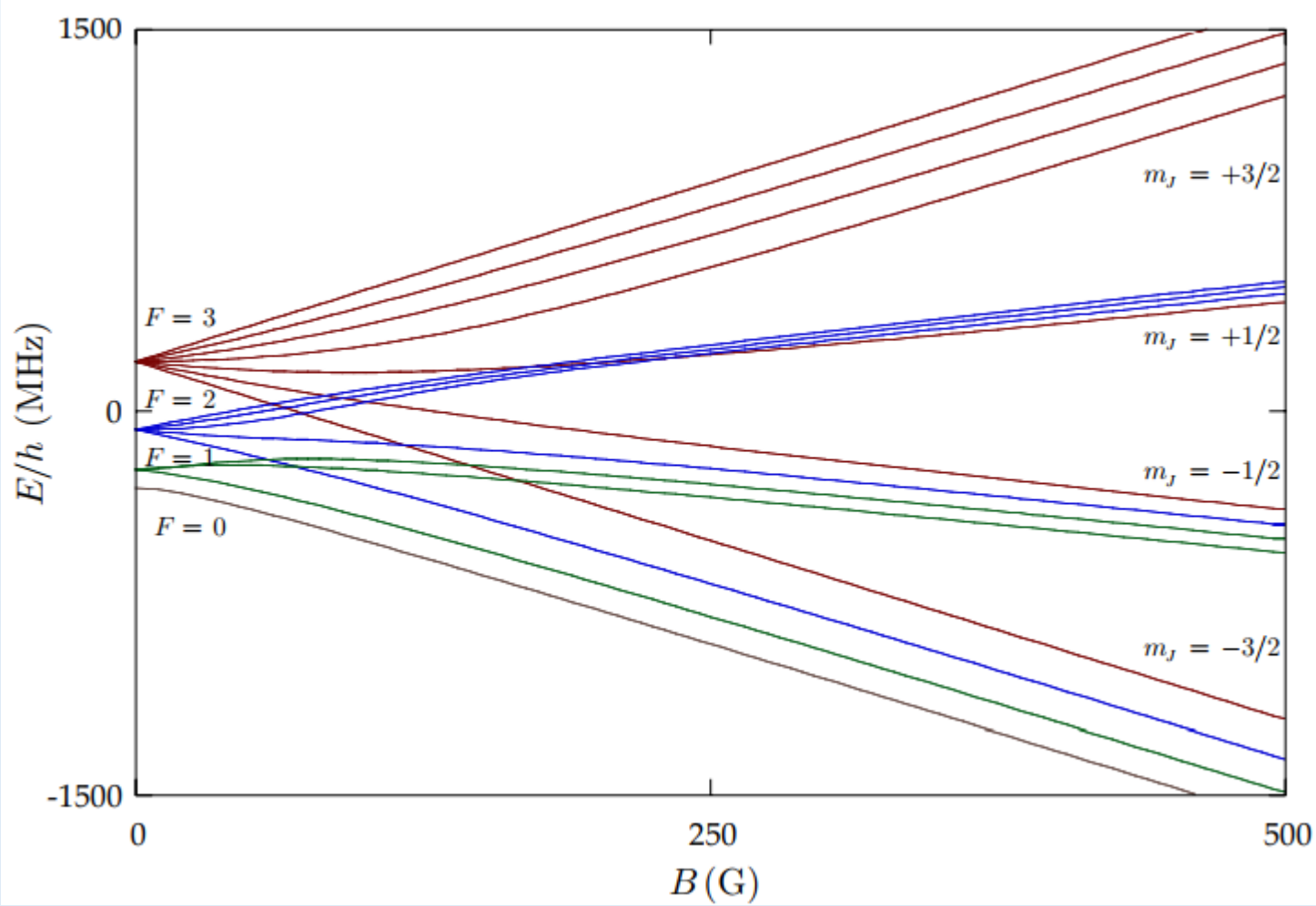

rubidium-87 $P_{3/2}$ states, ~84 MHz splitting

Daniel Steck

Looking ahead: Atoms in static (E) fields

The dc Stark effect
interaction of electron with static E-field mixes states of opposite parity (s-p, p-d, etc.)

This effect induces a dipole moment, leading to a charge asymmetry, and leads to the formation of things like bonding orbitals when the "field" applied is actually just due to the presence of a nearby atom
(as in molecules and in solids)

The dc Stark effect isn't so crucial to most experiments, as the typical neutral atom is pretty hard to polarize (need ~ GV/cm fields). This can be important for Rydberg atoms and molecules, and in quenching metastable states

This small mixing will be **really** important to our discussion of electric dipole transitions

Added reading, controlling ΔE(B)

Clock state spectroscopy

Ketterle group,
Gretchen Campbell

increased, presumably because of the larger onsite interaction energy as the lattice trap was increased. As given in Eq. 7, the separation between the peaks provides a direct measurement of the onsite interaction energy, U. Our results are in good agreement with calculated values of U (Fig. 2A). Although the separation between the $n = 1$, $n = 2$, and $n = 3$ peaks is roughly constant, for higher filling factors the separation between the peaks decreases; the effective onsite interaction energy becomes smaller for higher filling factors (Fig. 2B). This result shows that for low occupation numbers the atoms occupy the ground state wave function of the lattice site, whereas for larger occupation numbers, the repulsive onsite interaction causes the wave function to spread out, lowering the interaction energy. From a variational calculation of the wave function similar to (*17*), we

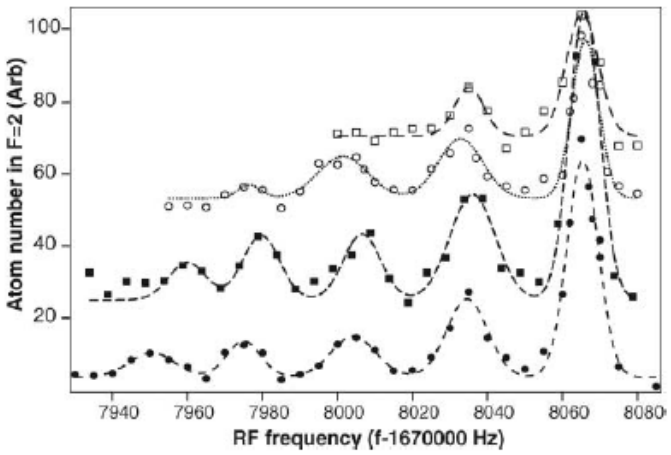

Fig. 4. Lifetime of individual MI shells. The lifetime for each MI phase can be measured independently by adding a hold time before applying the two-photon pulse. Spectra are shown for hold times of 0 ms (solid circles), 100 ms (solid squares), 400 ms (open circles), and 2000 ms (open squares). The lattice depth was $V = 35E_{rec}$ except for the 100-ms hold time, for which it was $V = 34E_{rec}$. The lines show Gaussian fits to the peaks, and the spectra were offset for clarity.

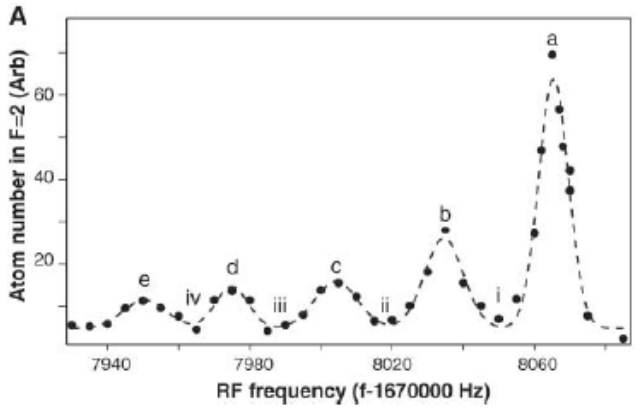

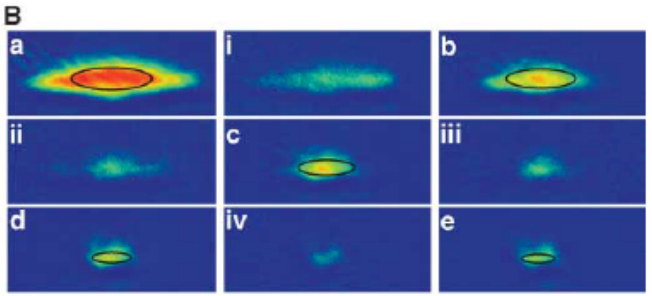

Fig. 3. Imaging the shell structure of the MI. (**A**) Spectrum of the MI at $V = 35E_{rec}$. (**B**) Absorption images for for decreasing rf frequencies. Images a to e were taken on resonance with the peaks shown in (A) and display the spatial distribution of the $n = 1$ to $n = 5$ shells. The solid lines shows the predicted contours of the shells. Absorption images taken for rf frequencies between the peaks (images i to iv) show a much smaller signal. The field of view was 185 μm by 80 μm.